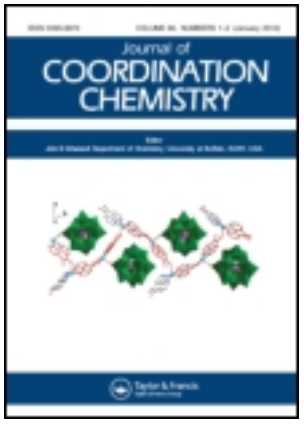

Journal of Coordination Chemistry
Publication details, including instructions for authors and subscription information:
http://www.tandfonline.com/loi/gcoo20

Synthesis and characterization of a large bite angle xantphos iridium complex

Thashree Marimuthu [a], Muhammad D. Bala [a] & Holger B. Friedrich [a]

[a] School of Chemistry & Physics, University of KwaZulu-Natal, Durban, South Africa

Accepted author version posted online: 22 Jan 2013.Published online: 05 Mar 2013.

To cite this article: Thashree Marimuthu, Muhammad D. Bala & Holger B. Friedrich (2013) Synthesis and characterization of a large bite angle xantphos iridium complex, Journal of Coordination Chemistry, 66:5, 780-788, DOI: 10.1080/00958972.2013.769212

To link to this article: http://dx.doi.org/10.1080/00958972.2013.769212

Journal of Coordination Chemistry
Vol. 66, No. 5, 10 March 2013, 780–788

Synthesis and characterization of a large bite angle xantphos iridium complex

THASHREE MARIMUTHU, MUHAMMAD D. BALA* and HOLGER B. FRIEDRICH*

School of Chemistry & Physics, University of KwaZulu-Natal, Durban, South Africa

(*Received 23 August 2012; in final form 3 December 2012*)

The xantphos iridium complex [Ir(xantphos)(H)(CO)(PPh_3)] CH_2Cl_2 (**3**) was synthesized and structurally characterized by NMR, IR, and single-crystal X-ray diffraction. Complex **3** crystallizes with two molecules (A,B) in the asymmetric unit. The coordination around Ir is trigonal bipyramidal with all three P groups occupying equatorial positions. The carbonyl and hydride occupy axial sites. This mode of bonding results in a complex that exhibited large bite (P1–Ir–P2) angles of 109.12(6) and 110.50(6)° for the A and B molecules, respectively. NMR data further support the structural elucidation of **3** and IR data confirm the presence of Ir bound to both a carbonyl and a hydride. Thermal analyses of **3** indicate that it is thermally stable up to >400 °C under nitrogen.

Keywords: Xantphos; Diphosphine; Iridium complex; Bite angle; Catalyst

1. Introduction

Phosphines are popular ligands in organometallic chemistry and homogeneous catalysis due to their versatility and ability to stabilize the coordination environment, and therefore influence the reactivity of metal complexes. An area of continuing interest is probing the influence of phosphine ligands on transition metal centers [1–4]. For monophosphines, the Tolman cone angle θ can be calculated to estimate the space that the ligand occupies around the metal center [5]. If X-ray crystal structure is not available, computational modeling can be used to calculate such molecular descriptors [6]. For example, the natural bite angle introduced by Casey and Whiteker [7] has been applied to different classes of diphosphine ligands. Xantphos (**1**) belongs to a family of diphosphines that are characterized by a common xanthene backbone. The natural bite angle of xantphos is 111.7° and, as a consequence, its complexes have relatively large bite angles as well. Several xantphos-based complexes of Pd [8–13], as well as a few of Ru [14–18] and Rh [19, 20], have been characterized by X-ray crystallography. However, to the best of our knowledge, only Eisenberg and co-workers [21] have reported halide derivatives of Ir carbonyl complexes based on xantphos. We previously reported Ir(nixantphos) [22], a POP derivatized nixantphos ligand [23], and three xantphos-related ligands [24]. Herein, we report an Ir xantphos hydride complex that was easily prepared from a readily available Ir hydride precursor (scheme 1). Metal hydride complexes are important, but elusive, starting materials to the

*Corresponding authors. Email: bala@ukzn.ac.za (M.D. Bala); friedric@ukzn.ac.za (H.B. Friedrich)

Journal of Coordination Chemistry
ISSN 0095-8972 print/ISSN 1029-0389 online
http://dx.doi.org/10.1080/00958972.2013.769212

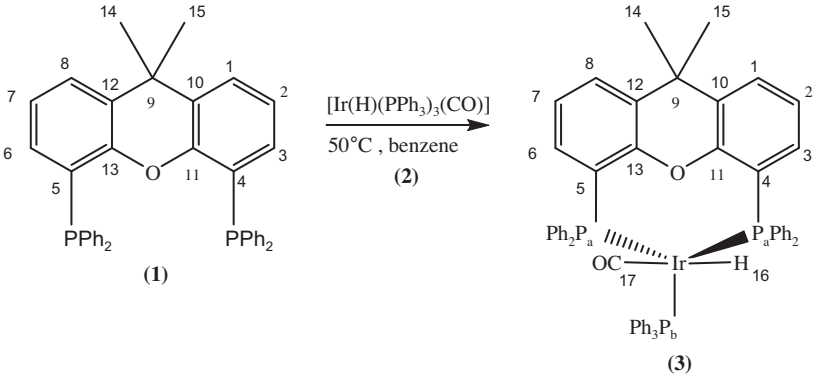

Scheme 1. Synthesis of complex **3** from xantphos ligand **1**.

generation of active catalysts used in many organic transformations. Hence, elucidation of their solid state configurations extends the scope of our understanding of their roles in catalysis.

2. Experimental

2.1. *Materials and methods*

Chemicals used were of reagent grade and reactions were carried out in distilled and dried solvents using standard Schlenk tube techniques. Xantphos was prepared from an adapted literature method [25]. Iridium trichloride hydrate ($IrCl_3 \cdot xH_2O$) was obtained from Johnson Matthey and used as received. The metal precursor was prepared via reported syntheses [26, 27]. FTIR spectra were recorded in the range 4000–400 cm^{-1} on a Perkin-Elmer infrared spectrophotometer coupled with an attenuated total reflectance accessory. ^{1}H-, ^{31}P-, and ^{13}C-NMR measurements were collected at 298 K with a Bruker AVANCE III 600 MHz spectrometer using 5 mm tubes and benzene–d_6 as solvent. Coupling constants (J) are given in Hz. The melting point was determined using a Gallenkamp melting point apparatus and is uncorrected. High resolution mass spectrometry was obtained with a Bruker micrOTOF-Q II instrument operating at ambient temperatures, under electron spray ionization conditions, based on a sample concentration of approximately 1 ppm. Differential scanning calorimetry (DSC) measurements (Al_2O_3 reference standard) were performed on a TA Thermo Gravimetric Analyzer at a heating rate of 10 °C/min under an atmosphere of nitrogen. Elemental analyses were performed on a LECO CHNS-932 elemental analyzer.

2.2. *Synthesis*

To $[Ir(H)(CO)(PPh_3)_3]$ (0.22 g, 0.22 mmol) in benzene (20 mL), xantphos (0.1 g, 0.17 mmol) was added. The resulting yellow solution was left to stir at 50 °C for 5 h. Thereafter, the solvent was reduced to half its volume, after which a yellow precipitate was formed, and the excess solvent was removed via a cannula. The yellow solid was first washed with methanol, then hexane and dried under vacuum. Complex **3** was

recrystallized from dichloromethane/hexane (1/1) to afford 79% (143 mg) of a yellow powder. Melting point in air: 463–465 K (decomposed) and DSC 523 K (under N_2).

2.3. *Structural analysis and refinement*

Single-crystal structure determination by X-ray diffraction was performed on a Bruker APEXII CCD area-detector diffractometer with graphite-monochromated Mo-*Kα* radiation using APEX 2 data collection software [28]. Data reduction was carried out using *SAINT–Plus*software [29] and face-indexed absorption corrections were made using *XPREP*. The crystal structure was solved by direct methods using *SHELXTL*. Non-hydrogen atoms were first refined isotropically followed by anisotropic refinement by full matrix least-squares based on F^2 using *SHELXTL*. Hydrogens were first located in the difference map then positioned geometrically and allowed to ride on their respective parent with C–H = 0.95 Å and $U_{iso}(H) = 1.2U_{eq}(C)$. Diagrams and publication material were generated using *SHELXTL* [30], PLATON [31], and ORTEP-3 [32]. Further details of the X-ray structural analysis are given in table 1, while selected bond lengths and angles for **3** are listed in table 2.

3. Results and discussion

3.1. *Synthesis*

Substitution of two PPh_3 on [Ir(H)(CO)(PPh_3)$_3$] (**2**) by bidentate xantphos resulted in the isolation of [Ir(xantphos)(H)(CO)(PPh_3)] (**3**) in good yield (scheme 1). Single crystals suitable for X-ray analysis were grown by slow diffusion of hexane into a dichloromethane solution of **3**.

3.2. *NMR data*

The NMR data for **3** are presented in table 3 and the atomic numbering in scheme 1. In the ^{1}H NMR spectrum of **3**, the aliphatic region contains two methyl signals at 1.44

Table 1. Crystal data and structure refinement for **3**.

Empirical formula	$C_{59}H_{50}Cl_2IrO_2P_3$
Formula weight	1147
Crystal system	Monoclinic
Space group	*P*21/*c*
a [Å], *b* [Å], *c* [Å]	24.3353(5), 37.9609(7), 11.0859(2)
β [°]	97.725(1)
Volume [Å^3]	10148.1(3)
Z	8
Density (calculated) [Mg m^{-3}]	1.502
Absorption coefficient [mm^{-1}]	2.874
F(0 0 0)	4608
Reflections collected	86,237
Independent reflections	24,378 [*R*(int) = 0.0633]
Goodness-of-fit on F^2	0.918
Final *R* indices [*I* > 2sigma(*I*)]	*R*1 = 0.0405, *wR*2 = 0.0818
R indices (all data)	R_1 = 0.0826, wR_2 = 0.0915

Table 2. Bond lengths [å] and angles [°] for **3**.

	Molecule			Molecule	
Bond lengths [å]	A	B	Bond angles [°]	A	B
P(1)–C(5)	1.838(7)	1.833(7)	P(1)–Ir(1)–P(2)	109.12(6)	101.50(6)
P(2)–C(4)	1.839(7)	1.844(7)	P(1)–Ir(1)–P(3)	122.29(6)	121.73(6)
P(1)–C(20)	1.834(8)	1.838(8)	P(2)–Ir(1)–P(3)	125.49(6)	124.53(6)
P(2)–C(40)	1.828(7)	1.841(8)	P(1)–Ir(1)–C(16)	95.8(2)	94.5(2)
P(3)–C(60)	1.836(7)	1.849(7)	P(2)–Ir(1)–C(16)	92.8(2)	94.4(2)
C(11)–O(1)	1.380(9)	1.380(9)	P(3)–Ir(1)–C(16)	98.5(2)	98.6(2)
C(13)–O(1)	1.389(8)	1.388(8)	H(17)–Ir(1)–P(1)	82.2(2)	78(3)
C(9)–C(10)	1.516(10)	1.515(10)	H(17)–Ir(1)–P(2)	86.2(2)	86(3)
C(9)–C(14)	1.525(10)	1.524(11)	H(17)–Ir(1)–P(3)	84.2(2)	88(3)
Ir(1)–H(17)	1.55(6)	1.05(5)	C(5)–P(1)–Ir(1)	112.8(2)	113.3(2)
C(16)–O(2)	1.143(9)	1.172(9)	C(4)–P(2)–Ir(1)	113.2(2)	112.6(2)
Ir(1)–C(16)	1.886(7)	1.858(7)	C(20)–P(1)–C(30)	100.5(3)	100.7(3)
Ir(1)–P(1)	2.3121(17)	2.2982(17)	C(40)–P(2)–C(50)	102.0(3)	101.6(3)
Ir(1)–P(2)	2.3050(17)	2.3034(19)	C(10)–C(9)–C(12)	105.5(6)	104.5(6)
Ir(1)–P(3)	2.2850(18)	2.2863(18)	C(11)–O(1)–C(13)	112.6(5)	112.7(5)

Table 3. NMR spectroscopic data for **3**.

[a]Carbon no.	^{1}H (=ppm)	^{13}C (=ppm)
1, 8	6.75 (t, 3J(H,H) = 7.7 Hz, 2H)	122.9
2, 7	7.07 (dd, 3J(H,H) = 7.6, 2J(P,H) = 1.1 Hz, 2H)	125.0
3, 6	6.73–6.66 (m, 2H)	130.2
4, 5	–	127.4 (d, J(P,C) = 9.7 Hz)
9	–	36.1
12, 10	–	135.2
13, 11	–	156.3 (t, J(P,C) = 4.5 Hz)
14	1.44	24.3
15	1.35	29.0
Phenyl groups on Pa	6.99–6.80 (m, 20H)	136.8 (td, J(P,C) = 22.1, 2.8 Hz), 133.7 (t, J(P,C) = 6.4 Hz), 133.5 (m)
Phenyl groups on Pb	7.74 (m, 4H), 7.66–7.57 (m, 6H), 7.45 (m, 4H)	133.4 (m), 130.2 (m), 128.1 (m)
CO	–	189.9 (weak)

Note: [a]Carbon numbers relative to the numbering scheme for **3** in scheme 1.

and 1.35 ppm, because upon complexation to iridium, methyl groups at C14 and C15 tilt away from each other to minimize steric interactions. A triplet at $\delta = 6.75$ ppm, a doublet of doublets at 7.07 ppm, and a multiplet at 6.73–6.66 ppm are assigned to the neighboring xanthene protons due to an ABCXX″ system where X and $X'' = {}^{31}$P.

The heteronuclear single quantum coherence NMR spectrum (HSQC, figure 1) confirms assignments of ^{13}C signals for C1,8, C2,7, and C3,6 at $\delta = 122.9$, 125.0, and 130.2 ppm, respectively. Multiplets between 6.99 and 6.80 ppm integrating for 20 protons were assigned to aromatic protons of the phosphine donors (P_a). The corresponding signals in the ^{13}C NMR spectrum were assigned using 2D heteronuclear multiple-bond correlation spectroscopy and are presented in table 3, with the P–C_{ipso} signal observed extremely downfield at 141.4 ppm. This deshielding is expected due to the electronic effect of phosphorus. Similarly, signals for phenyls on P_b are assigned as summarized in table 3. The remaining fully substituted carbons of the xanthene ring C13,11; C12,10; and C4,5 are assigned to a triplet at 156.3, a singlet at 135.2, and a doublet at 127.4 ppm, respectively.

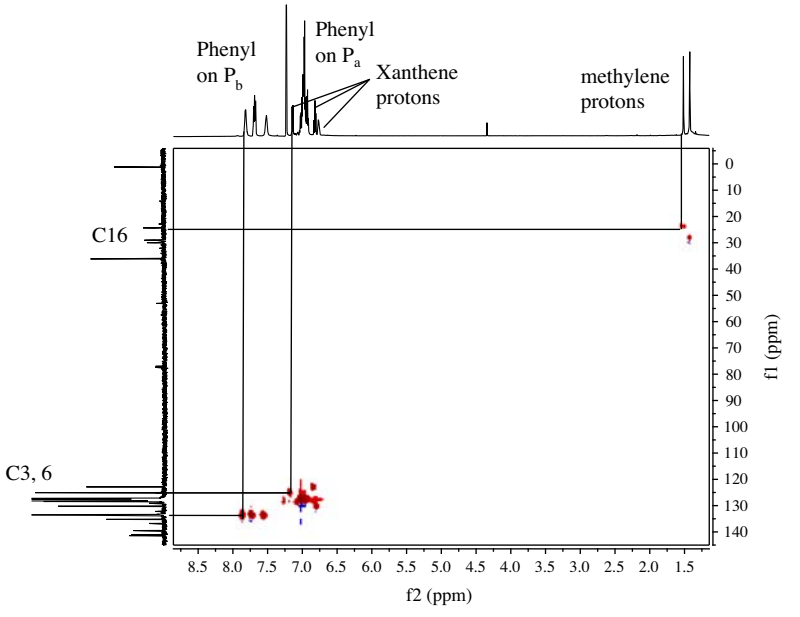

Figure 1. HSQC NMR spectrum of **3** in C_6D_6.

A very weak signal at $\delta = 189.9$ ppm is indicative of the carbonyl bound to Ir. In the ^{1}H NMR spectrum, a doublet of triplets significantly shifted upfield at −10.5 is diagnostic of the metal hydride [figure 2(a)]. The coupling constants of $J(P_a, H) = 26.2$ and $J(P_b, H) = 19.6$ Hz, 1H are small and similar to the values obtained for [Ir(BDNA)(H)(CO)(PPh$_3$)], suggesting that the hydride is *cis* to all three phosphines [33]. The X-ray crystal structure confirms this.

In the ^{31}P NMR [figure 2(b)], the triplet at 16.52 ($JP_bP_a = 137.1$ Hz) suggests that the two equivalent phosphines (P_a) of the bidentate phosphine couple with P_b of PPh_3. Likewise, a doublet at −1.50 ppm ($JP_aP_b = 138.7$ Hz) [figure 2(b)] is assigned to P_a. The relatively large coupling constant found for **3** is similar to that reported for P_a ($JP_aP_b = 119.1$) and P_b ($JP_bP_a = 119.1$) in [Rh(xantphos)(H)(CO(PPh$_3$)] [25].

3.3. *Mass spectrometry (high resolution), elemental (CHN) and differential scanning calorimetric (DSC) analyses*

The exact mass for **3**, $C_{58}H_{49}IrO_2P_3$, was calculated as 1063.2569. The mass spectrum of **3** shows the highest intensity molecular peak at $m/z = 1063.2569$ for the positively charged adduct $[Ir(xantphos)(CO)(PPh_3)(H)]^+$, together with several isotopic peaks, from $m/z = 1061.2549$ to 1067.2452, with adjacent peaks separated by 1 m/z. The observed isotope distribution pattern shows an envelope of peaks, which is characteristic of a monocation [34]. The elemental analyses for **3** (mass calculated for $C_{58}H_{48}IrO_2P_3$: C, 65.6; H, 4.6; found: C, 65.7; H, 4.4) are indicative of good bulk purity of the complex. The DSC under nitrogen revealed an exotherm representing crystallization at 225 °C and the melting point was observed as an endotherm at 250 °C. The DSC results indicate that the complex has good thermal stability with the onset of decomposition at temperatures

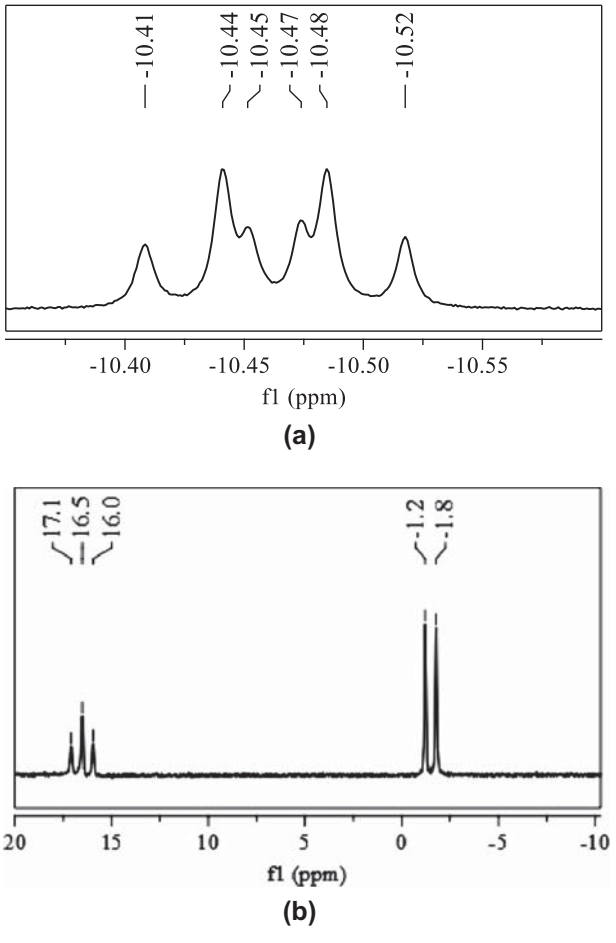

Figure 2. (a) Expanded ^{1}H NMR spectrum and (b) ^{31}P NMR of **3** in C_6D_6.

higher than 400 °C, as compared to the decomposition observed when the sample was heated to 190 °C in air.

3.4. *IR data*

The IR absorption peak of the carbonyl in **3** appeared at a higher wavenumber 1923 cm^{-1} as compared to 1917 cm^{-1} observed for the carbonyl absorption of **2**, suggesting that back donation from iridium to the π^* molecular orbital of CO was lower than for the precursor complex. If the strong electron donating PPh_3 was coordinated *trans* to CO, then the IR absorption peak of the carbonyl group would appear at a lower wavenumber due to higher back donation of electron density to the π^* orbital of the CO ligand. A strong band indicative of Ir–H absorption was observed at 2057 cm^{-1}. This value indicates a weaker Ir–H bond as compared to the band found in **2** (2120 cm^{-1}), possibly resulting in a more catalytically active complex. A weak aromatic CH stretch at 3056 cm^{-1} and the medium carbon-carbon stretch bands between 1478 and 1585 cm^{-1} are diagnostic of the aromatic

rings found in the ligand backbone of **3**. The bands for CH bends are observed at 1088 cm^{-1} for the in-plane bends, and at 692 cm^{-1} for the out-of-plane bends.

3.5. *X-ray diffraction data*

The geometry around the Ir center in **3** is a distorted trigonal bipyramid of ligands with all three P donors occupying equatorial sites (figure 3). Ir is located only slightly above the equatorial plane defined by the three phosphorus donors and displaced toward the apical carbonyl. The P–Ir–C16 angles range from 92.8(2) to 98.5(2)° for molecule A and from 94.4(2) to 98.6(2)° for molecule B. These values indicate that the phosphine ligands are close to the hydride which is *trans* to the carbonyl to reduce steric repulsion caused by the interaction between the carbonyl and phosphines. Hence, Ir lies above the equatorial plane. Similarly, bond angle values from 94.9(4) to 98.0(4)° were reported for [Ir(Cl)(CO)$(H)_2$(xantphos)] [21] which also contained hydride *trans* to CO.

Bond angles involving P1–Ir–P2 for **3** are 109.12(6)° for molecule A and 110.50(6)° for molecule B. The large bite angle also results in large P1–Ir–P3 and P2–Ir–P3 angles. The observed P1–Rh–P2 bite angles reported for related crystal structures of [Rh(nixantphos)(H)(CO)(PPh_3)] and [Rh(benzoxantphos)(H)(CO)(PPh_3)] are 110.21(3) and 109.16(5)°, respectively [35]. This supports the claim that the ligands fall into a homologous family of ligands where only minor differences in the bite angle are observed upon changing the transition metal. However, the bite angles reported for [Ir(X)$(CO)_2$(xantphos)], where X = I, Br, Cl, were 100.287(13), 103.03(2), and 100.008(18)°, respectively [21]. In this

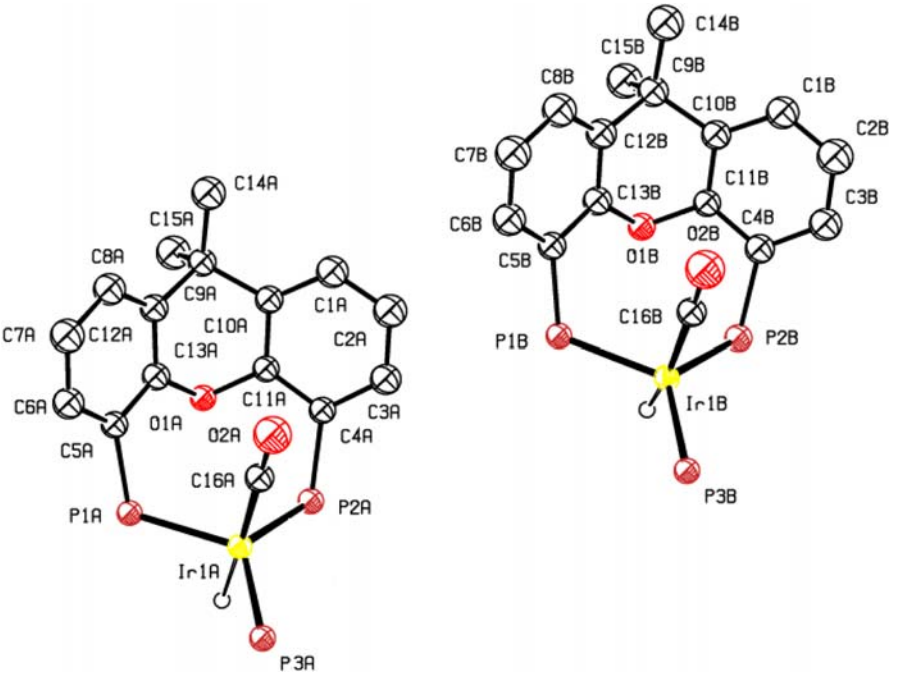

Figure 3. ORTEP drawing of **3** showing the atom numbering scheme. Thermal ellipsoids are shown at 50% probability with hydrogens and phenyls omitted to emphasize the coordination around Ir.

instance, although the metal center is the same, the different steric properties of the counter ligands gave a range of smaller bite angles when compared to **3**.

The xanthene is bent in a bowl conformation, significantly distorted from planarity, resulting in relatively large dihedral angles in the molecules A [47.94(2)°] and B [48.32 (2)°]. Compared to free ligand [23.43(2)°], the folding of the backbone was nearly doubled in **3** to accommodate coordination to the metal center [25]. The solid state depiction of the positions of hydride in both A and B is not absolute; however, the crystal structure confirmed the assignments in the ^{1}H NMR and IR spectra.

All three Ir–P bond distances [2.29–2.31 Å for molecule A and 2.29–2.30 Å for molecule B] are within the range of values [2.24–2.28 Å] found in [Ir(BDNA)(H)(CO)PPh_3)] [33] [BDNA = 1,8-bis(diphenylphosphinomethyl)naphthalene] and [2.37–2.38 Å] reported for [Ir(H)$(CO)_2PPh_3)_2$] [36].

4. Conclusions

The new iridium complex [Ir(xantphos)(H)(CO)(PPh_3)] has been synthesized and fully characterized. Through analysis of NMR and single-crystal X-ray diffraction data, the coordination around Ir is established as trigonal bipyramidal with all three P groups bound equatorially, and the carbonyl and hydride occupying apical sites.

Supplementary material

Crystallographic data for the structure in this article have been deposited with the Cambridge Crystallographic Data Center, CCDC 895,753. This data can be obtained free of charge at http://www.ccdc.cam.ac.uk/conts/retrieving.html or from the Cambridge Crystallographic Data Center, 12 Union Road, Cambridge CB2 1EZ, UK; Fax: +44 1223/336 033; E-mail: deposit@ccdc.cam.ac.uk.

Acknowledgments

We wish to thank Dr. Manuel Fernandes (University of the Witwatersrand) for crystal data collection, SASOL, THRIP, and the University of KwaZulu-Natal for the financial support. We gratefully acknowledge Johnson Matthey for a loan of iridium trichloride.

References

[1] C.A. Tolman. *Chem. Rev.*, **77**, 313 (1977).
[2] A. Schnyder, T. Aemmer, A.F. Indolese, U. Pittelkow, M. Studer. *Adv. Synth. Catal.*, **344**, 495 (2002).
[3] Z. Freixa, M.S. Beentjes, G.D. Batema, C.B. Dieleman, G.P.F. van Strijdonck, J.N.H. Reek, P.C.J. Kamer, J. Fraanje, K. Goubitz, P.W.N.M. van Leeuwen. *Angew. Chem. Int. Ed.*, **42**, 1284 (2003).
[4] L. Lan-Chang. *Coord. Chem. Rev.*, **250**, 1152 (2006).
[5] C.A. Tolman. *J. Am. Chem. Soc.*, **92**, 2956 (1970).
[6] J.A. Gillespie, D.L. Dodds, P.C.J. Kamer. *Dalton Trans.*, **39**, 2751 (2010).
[7] C.P. Casey, G.T. Whiteker. *Israel J. Chem.*, **30**, 299 (1990).
[8] M. Kranenburg, J.G.P. Delis, P.C.J. Kamer, P.W.N.M. van Leeuwen, K. Vrieze, N. Veldman, A.L. Spek, K. Goubitz, J. Fraanje. *J. Chem. Soc. Dalton Trans.*, 1839 (1997).

[9] J. Yin, S.L. Buchwald. *J. Am. Chem. Soc.*, **124**, 6043 (2002).
[10] M.A. Zuideveld, B.H.G. Swennenhuis, M.D.K. Boele, Y. Guari, G.P.F. van Strijdonck, J.N.H. Reek, P.C.J. Kamer, K. Goubitz, J. Fraanje, M. Lutz, A.L. Spek, P.W.N.M. van Leeuwen. *J. Chem. Soc.. Dalton Trans.*, 2308 (2002).
[11] L.M. Klingensmith, E.R. Strieter, T.E. Barder, S.L. Buchwald. *Organometallics*, **25**, 82 (2005).
[12] V.V. Grushin, W.J. Marshall. *J. Am. Chem. Soc.*, **128**, 12644 (2006).
[13] A.M. Johns, M. Utsunomiya, C.D. Incarvito, J.F. Hartwig. *J. Am. Chem. Soc.*, **128**, 1828 (2006).
[14] P. Nieczypor, P.W.N.M. van Leeuwen, J.C. Mol, M. Lutz, A.L. Spek. *J. Organomet. Chem.*, **625**, 58 (2001).
[15] A.E.W. Ledger, P.A. Slatford, J.P. Lowe, M.F. Mahon, M.K. Whittlesey, J.M.J. Williams. *Dalton Trans.*, 716 (2009).
[16] B. Deb, B.J. Borah, B.J. Sarmah, B. Das, D.K. Dutta. *Inorg. Chem. Commun.*, **12**, 868 (2009).
[17] B. Deb, D.K. Dutta. *Polyhedron*, **28**, 2258 (2009).
[18] A.N. Kharat, A. Bakhoda, B.T. Jahromi. *Inorg. Chem. Commun.*, **14**, 1161 (2011).
[19] A.J. Sandee, L.A. van der Veen, J.N.H. Reek, P.C.J. Kamer, M. Lutz, A.L. Spek, P.W.N.M. van Leeuwen. *Angew. Chem. Int. Ed.*, **38**, 3231 (1999).
[20] J.W. Faller, S.C. Milheiro, J. Parr. *J. Organomet. Chem.*, **693**, 1478 (2008).
[21] D.J. Fox, S.B. Duckett, C. Flaschenriem, W.W. Brennessel, J. Schneider, A. Gunay, R. Eisenberg. *Inorg. Chem.*, **45**, 7197 (2006).
[22] T. Marimuthu, M.D. Bala, H.B. Friedrich. *J. Coord. Chem.*, **62**, 1407 (2009).
[23] T. Marimuthu, M.D. Bala, H.B. Friedrich. *Acta Crystallogr., Sect. E*, **64**, O1984–U4311 (2008).
[24] T. Marimuthu, M.D. Bala, H.B. Friedrich. *J. Chem. Crystallogr.*, **42**, 251 (2012).
[25] M. Kranenburg, Y.E.M. Vanderburgt, P.C.J. Kamer, P.W.N.M. van Leeuwen, K. Goubitz, J. Fraanje. *Organometallics*, **14**, 3081 (1995).
[26] N. Ahmad, J.J. Levison, S.D. Robinson, M.F. Uttley. Complexes of Ruthenium, Osmium, Rhodium, and Iridium Containing Hydridearbonyl, or Nitrosyl Ligands. In Inorganic Syntheses, G.W. Parshall (Ed.), pp. 45–64, McGraw-Hill, New York, NY (1974).
[27] N. Ahmad, S.D. Robinson, M.F. Uttley. *J. Chem. Soc., Dalton Trans.*, 843 (1972).
[28] Bruker, APEX2. Version 2009.1-0. Bruker AXS Inc., Madison, Wisconsin, USA (2005).
[29] Bruker, SAINT+. Version 7.60A. (Includes XPREP and SADABS) Bruker AXS Inc., Madison, Wisconsin, USA (2005).
[30] G.M. Sheldrick. *Acta Crystallogr., Sect. A*, **64**, 112 (2008).
[31] A.L. Spek. *J. Appl. Cryst.*, **36**, 7 (2003).
[32] L.J. Farrugia. *J. Appl. Cryst.*, **30**, 565 (1997).
[33] R.-X. Li, X.-J. Li, N.-B. Wong, K.-C. Tin, Z.-Y. Zhou, T.C.W. Mak. *J. Mol. Catal. A: Chem.*, **178**, 181 (2002).
[34] W. Henderson, J.S. McIndoe. *Mass Spectroscopy of Inorganic, Coordination and Organometallic Compounds*. p. 128, Wiley, Chichester (2005).
[35] L.A. van der Veen, P.H. Keeven, G.C. Schoemaker, J.N.H. Reek, P.C.J. Kamer, P.W.N.M. van Leeuwen, M. Lutz, A.L. Spek. *Organometallics*, **19**, 872 (2000).
[36] M. Ciechanowicz, A.C. Skapski, P.G.H. Troughton. *Acta Crystallogr., Sect. B*, **32**, 1673 (1976).